

Production of Mesoporous Activated Carbon from Tea Fruit Peel Residues and Its Evaluation of Methylene Blue Removal from Aqueous Solutions

Junjie Gao,^a Dedong Kong,^b Yuefei Wang,^a Jing Wu,^a Shili Sun,^c and Ping Xu^{a,*}

Removal of methylene blue by activated carbon produced from tea fruit peel (*Camellia sinensis* L.) residue using agents ZnCl₂ (AC-1) and H₃PO₄ (AC-2) was investigated in this work. Mesoporous activated carbons with desirable surface areas and total pore volumes were obtained. Meanwhile, the characteristics of the activated carbon were examined. The effects of solution pH (2 to 10), contact time (0 to 480 min), and adsorbate dosage (0.5 to 3.5 g L⁻¹) were studied. Equilibrium adsorption data were found to be in good agreement with the Langmuir isotherm model. The maximum monolayer adsorption capacities of methylene blue onto activated carbons were 291.5 and 342.5 mg g⁻¹ for AC-1 and AC-2, respectively. The intraparticle diffusion model indicated that intraparticle diffusion was not the sole rate-determining step. The results demonstrated that the easily available tea fruit peel activated carbon is an excellent adsorbent for the removal of methylene blue from aqueous solutions.

Keywords: Activated carbon; Tea fruit peel; Removal; Methylene blue

Contact information: a: Department of Tea Science, Zhejiang University, 866 Yuhangtang Road, Hangzhou 310058, P. R. China; b: Agricultural Experiment Station of Zhejiang University, Hangzhou 310029, P. R. China; c: Tea Research Institute, Guangdong Academy of Agricultural Sciences, Guangzhou, Guangdong, 510640, P.R. China; *Corresponding author: zdxp@zju.edu.cn

INTRODUCTION

A considerable amount of dyes are being released into the hydrosphere due to their extensive use as coloring agents in many industries, such as textiles, printing, leather, cosmetics, paper, plastics, and even the dyestuffs industry itself (Crini 2006; Garg *et al.* 2004). Recent studies indicate that approximately 12% of synthetic dyes are lost during manufacturing and processing operations (Demirbas 2009). Synthetic dye has become one of the primary classes of pollutants in wastewater, owing to the high solubility of many dyes (Gupta 2009; Kyzas *et al.* 2012). The presence of dyes in effluents is not only undesirable aesthetically, but also poses a potential threat to the environment. It is known that dyes in the water inhibit sunlight penetration and reduce photosynthetic reactions (Wang *et al.* 2005). Above all, dyes are known for their toxicity and carcinogenicity toward human beings. Accordingly, to protect humans and recover ecosystems from contamination, dyes must be eliminated from dye-containing wastewater before being released into the environment (Ma *et al.* 2011).

The available literature shows that adsorption is an efficient method, when compared with other techniques, for re-using water in terms of low cost, flexibility and simplicity of design, ease of operation, and insensitivity to toxic pollutants (Demirbas 2009; Ma *et al.* 2011). The sorbent used for dye removal is generally dominated by

activated carbon due to its excellent adsorption capacity, which is related to its large surface area, pore volume, and porosity (Ahmaruzzaman 2008). Despite wide acknowledgment of the benefits of activated carbon for the treatment of wastewater, its usage is constrained due to its high cost. If the sorbent was inexpensive and ready for use, the activated carbon adsorption process would be regarded as a more attractive technology (Wang *et al.* 2005). Hence, research should focus on the exploration of economical activated carbon, ranging from the precursors to the methods of preparation, taking into consideration the urgent demand for activated carbon in wastewater treatment.

Recently, the evaluation of waste biomass is gaining attention all over the world, as it is renewable, widely available, cheap, and environmentally friendly (Karagöz *et al.* 2008). For example, agro-industrial byproducts are promising precursors for the preparation of activated carbon. Utilization of agricultural residues, such as oil palm fiber (Foo and Hameed 2011b), sunflower oil cake (Karagöz *et al.* 2008), cashew nut shell (Kumar *et al.* 2011), cotton stalk (Deng *et al.* 2009), jute fiber (Senthilkumaar *et al.* 2005), dead *Posidonia oceanica* leaves (Dural *et al.* 2011), and pine wood powder (Wang *et al.* 2009), as precursors for the preparation of activated carbon have been reported in the last few years. The popularity of tea (*Camellia sinensis* L.) seed oil, which has long been recognized as an edible oil of high quality, has been quickly increasing in the past few years. Consequently, the amount of residual tea fruit peel, the main byproduct of the manufacture of tea seed oil, has also increased. However, tea fruit peel is not typically utilized and the majority of it is discarded as industrial waste. This results in the loss of a valuable resource, as well as environmental pollution. Our previous work has revealed that phenolic-enriched extracts from tea fruit peel have remarkably high antioxidant activity and could potentially be developed as natural antioxidants and the extraction conditions has been optimized further. The residue of tea fruit peels after phenol extraction has not been explored extensively.

Therefore, in this work, the residue of tea fruit peel after phenol extraction was considered a candidate for the production of activated carbon. Activated carbons were prepared by a one-step method using the chemical agents $ZnCl_2$ and H_3PO_4 . Additionally, their potential application for methylene blue removal from an aqueous solution was investigated. Kinetic and equilibrium adsorption experiments were carried out to study adsorption behaviors in order to optimize the adsorption system.

EXPERIMENTAL

Materials and Methods

Preparation of activated carbon

Tea fruit was collected from Panban tea garden (Zhejiang, China) and washed in distilled water three times prior to separating the peel. The residues of tea fruit peel were dried at 110 °C for 12 h, ground, and sieved to a particle size range between 40 and 60 mesh. The processed raw material was soaked in $ZnCl_2$ solution and H_3PO_4 solution with an impregnation ratio of 1:1 (wt%), respectively, for 24 h, and the slurry was dried at 110 °C for 6 h. The dried mixture was put into a furnace and heated to 500 °C at a rate of 20 °C min^{-1} under a constant N_2 (99.99%) flow of 120 $cm^3 min^{-1}$. The activation process was maintained for 40 min. The activated substance was then successively washed with 0.1 N HCl and distilled water repeatedly until the pH was neutral. Finally, the product was dried at 110 °C for 8 h, ground, and sieved to a particle size of 180 mesh for further

analysis. The yield of activated carbon is defined as the weight after activation, washing, and drying. The percent yield was calculated by,

$$\text{Yield (\%)} = \frac{m}{M} \times 100 \quad (1)$$

where m and M are the dry weight (g) of the activated carbon and the dry weight (g) of the precursor, respectively.

Adsorbate

Methylene blue (MB), a common dye, was chosen for the adsorption experiments. Stock solution of 500 mg L⁻¹ dye was prepared by dissolving an accurate quantity of dye in distilled water. The required concentrations were obtained by diluting.

Characterization of activated carbon

Textural characterization of the activated carbon was measured by N₂ adsorption at 77 K (Autosorb-1-C Quantachrome, USA). Surface functional groups were examined using Fourier transform infrared (FT-IR) analysis (AVA TAR370, USA) with a scanning range of 4000 to 400 cm⁻¹. The surface morphology was detected by a scanning electron microscope (Hitachi S-3000N, Japan). The point of zero charge (pH_{pzc}) was determined according to the method described by Foo and Hameed (2011a).

Batch adsorption experiment

The effects of adsorption parameters, such as solution pH, adsorbate dosage, and contact time, were investigated. The investigation of the effect of solution pH was conducted by adding 0.04 g activated carbon into 50 mL of MB at a concentration of 400 mg L⁻¹ at different pH values (2 to 10) using a water bath shaker. The solution pH was adjusted by adding 0.1 N HCl and 0.1 N NaOH. The effect of adsorbate dosage was obtained by varying it from 0.5 g L⁻¹ to 3.5 g L⁻¹ with a MB concentration of 200 mg L⁻¹. The effect of contact time, varying from 0 to 480 min, was examined using a MB concentration of 300 mg L⁻¹ with a dosage of 2 g L⁻¹. The equilibrium adsorption study was completed by adding 0.025 mg activated carbon into 25 mL of different initial concentrations of MB. Kinetic adsorption studies were performed by adding 0.2 g activated carbon into 200 mL MB at a concentration of 200 mg L⁻¹. Aqueous samples were taken at pre-set time intervals and their concentrations were determined. For each experiment, agitation was conducted at a shaking speed of 120 rpm at a temperature of 25 °C and the final concentrations were filtered before they were measured by a UV-6100A spectrophotometer at the maximum absorption wavelength of 664 nm.

The amount of MB adsorption at equilibrium was calculated by,

$$q_e = (C_o - C_e) V / W \quad (2)$$

where C_o and C_e (mg/L) are the initial and equilibrium concentrations of MB, respectively, V (L) is the volume of the solution, and W (g) is the mass of adsorbents used.

The uptake of MB at time t , q_t (mg g⁻¹), was calculated by,

$$q_t = \frac{(C_0 - C_t)V}{W} \quad (3)$$

where C_t is the concentration of MB at any time.

The dye removal percentage was calculated as follows:

$$\text{Removal percentage (\%)} = \frac{(C_0 - C_e)}{C_0} \times 100 \quad (4)$$

RESULTS AND DISCUSSION

Yield

The yield of activated carbon is an important parameter, as it is closely associated with its commercial application. It can be seen from Table 1 that high yields (>46%) of activated carbon were obtained, which may be attributed to the activation agents and the relatively low temperature. It is acknowledged that phosphoric acid promotes the pyrolytic decomposition of the precursor and the formation of a cross-linked structure at relatively low temperatures (Ren *et al.* 2011). ZnCl_2 acts as a dehydrating agent, catalyzing the cleavage of hydroxyl groups present in the biopolymer and promoting the formation of double bonds inside the biopolymer chain and the biopolymer cleavage (Nieto-Delgado *et al.* 2011).

Table 1. Textural Characteristics, Yield, and pH_{pzc} of Activated Carbons

Sample	S_{BET} (m^2g^{-1})	V_{T} (cm^3g^{-1})	V_{Mic} (cm^3g^{-1})	V_{Mes} (cm^3g^{-1})	D_{Ap} (nm)	Yield (%)	pH_{pzc}
AC-1	1024	0.7463	0.2852	0.4631	2.915	47.38	2.120
AC-2	1320	0.7854	0.3234	0.4620	2.380	46.13	5.670

AC-1 and AC-2 are activated carbons produced by H_3PO_4 and ZnCl_2 , respectively
 S_{BET} = BET surface area, V_{T} = total pore volume, V_{Mic} = micropore volume, V_{Mes} = mesopore volume, D_{Ap} = average pore diameter

Characterization of Activated Carbon

It can be observed from Fig. 1 that the N_2 adsorption and desorption isotherm plots of AC-1 and AC-2 were quite different. According to the classification of IUPAC, the AC-1 adsorption isotherm was characteristic of type IV and the AC-2 adsorption isotherm was classified as an isotherm of type I, which was also known as the Langmuir isotherm, corresponding to its microporous character.

Micropore and mesopore size distributions of AC-1 and AC-2 are presented in Fig. 2, from which it can be found that activated carbon abundant with both micropores and mesopores was obtained. AC-2 displayed more micropores than AC-1, and such pores are essential to achieve high adsorption capacity. Table 1 shows the textural characteristics of activated carbons. It was found that the average pore diameters of AC-1 and AC-2 were 2.915 nm and 2.380 nm, respectively, indicating that they were mesoporous, based on the classification defined by the IUPAC. Pores are classified as micropores (<2 nm diameter), mesopores (2-50 nm diameter), and macropores (>50 nm diameter).

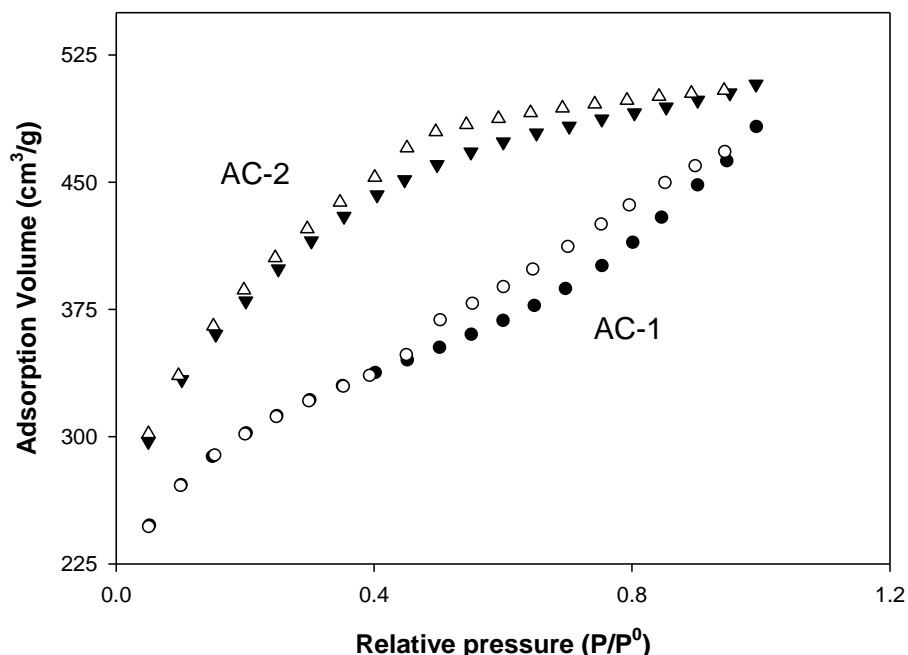


Fig. 1. N₂ adsorption and desorption isotherms at 77 K

The width, depth, and thickness of MB is 1.43, 0.61, 0.4 nm, respectively (Pelekani and Snoeyink 2000). Thus, it can be expected that the MB molecule has free access to the porous structure. Large surface areas, as well as high total volumes, were achieved with ZnCl₂ and H₃PO₄. However, AC-2 possessed greater surface areas than AC-1. This result may be due to acid washing, which removes ZnCl₂ more easily than H₃PO₄, reducing the possibility of activating agent deposition on the pores and sample surface (Liou 2010).

SEM photographs of activated carbons are presented in Fig. 3. Irregular apertures, which may be attributed to erosion caused by the H₃PO₄, are distributed on the rough surface (Fig. 3(a)). It was also observed that a honeycomb void structure, which is associated with high surface area and pore volume, had been developed (Fig. 3(b)).

FT-IR analysis was performed to examine the surface chemical functional groups of the samples. As shown in Fig. 4, the spectra of AC-1 and AC-2 shared similarities, though small peaks varied slightly. The peaks of all samples at around 3421 cm⁻¹ correspond to the O-H stretching vibrations, and the appearance of bands at around 1560 cm⁻¹ can be attributed to the stretching vibration of aromatic rings or C=C bonds (Ren *et al.* 2011). The small bond located at 1384 cm⁻¹ is assigned to C-H bending in alkane or alkyl groups (Cuhadaroglu and Uygun 2008). In the AC-1 spectrum, an evident peak at 1720 cm⁻¹ was observed, which is ascribed to the C=O group. An unambiguous assignment in the region of 1200 to 1000 cm⁻¹ is due to the overlap of absorption bands from many oxygen and phosphorous compounds (Baccar *et al.* 2009). In the AC-2 spectrum, C-O stretching, possibly attributed to phenol, caused the absorption at around 1220 cm⁻¹ (Sahu *et al.* 2010). The existence of such functional groups is considered to be connected with the mechanism in the adsorption process. Such mechanisms may include hydrogen bonding formation (-OH) (Vargas *et al.* 2011) as well as π - π dispersion interaction between the π -electrons of the aromatic compound MB and those of the graphene layers (Moreno-Castilla 2004).

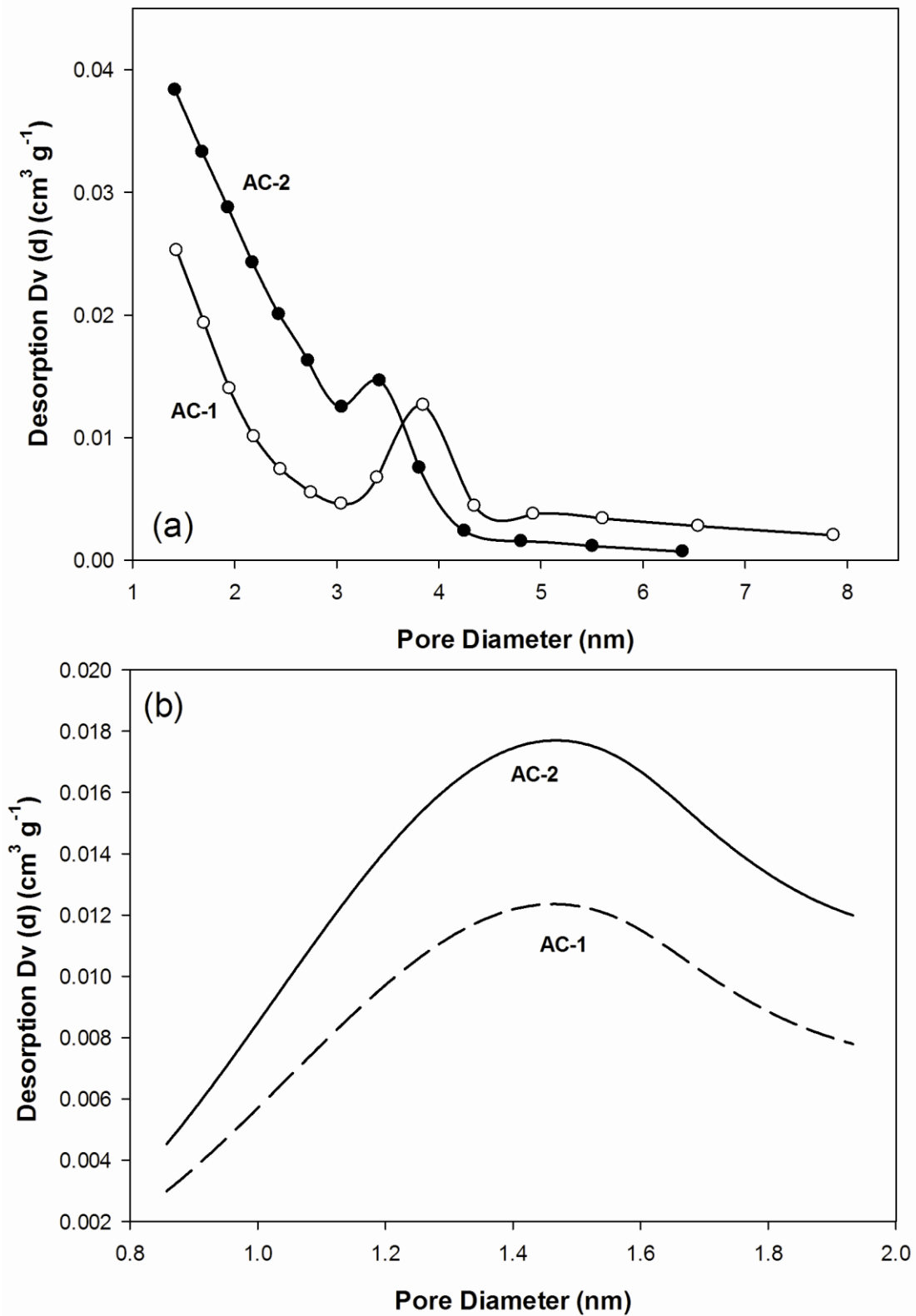


Fig. 2. (a) Mesopore size distribution by BJH method and (b) micropore size distribution by HK method

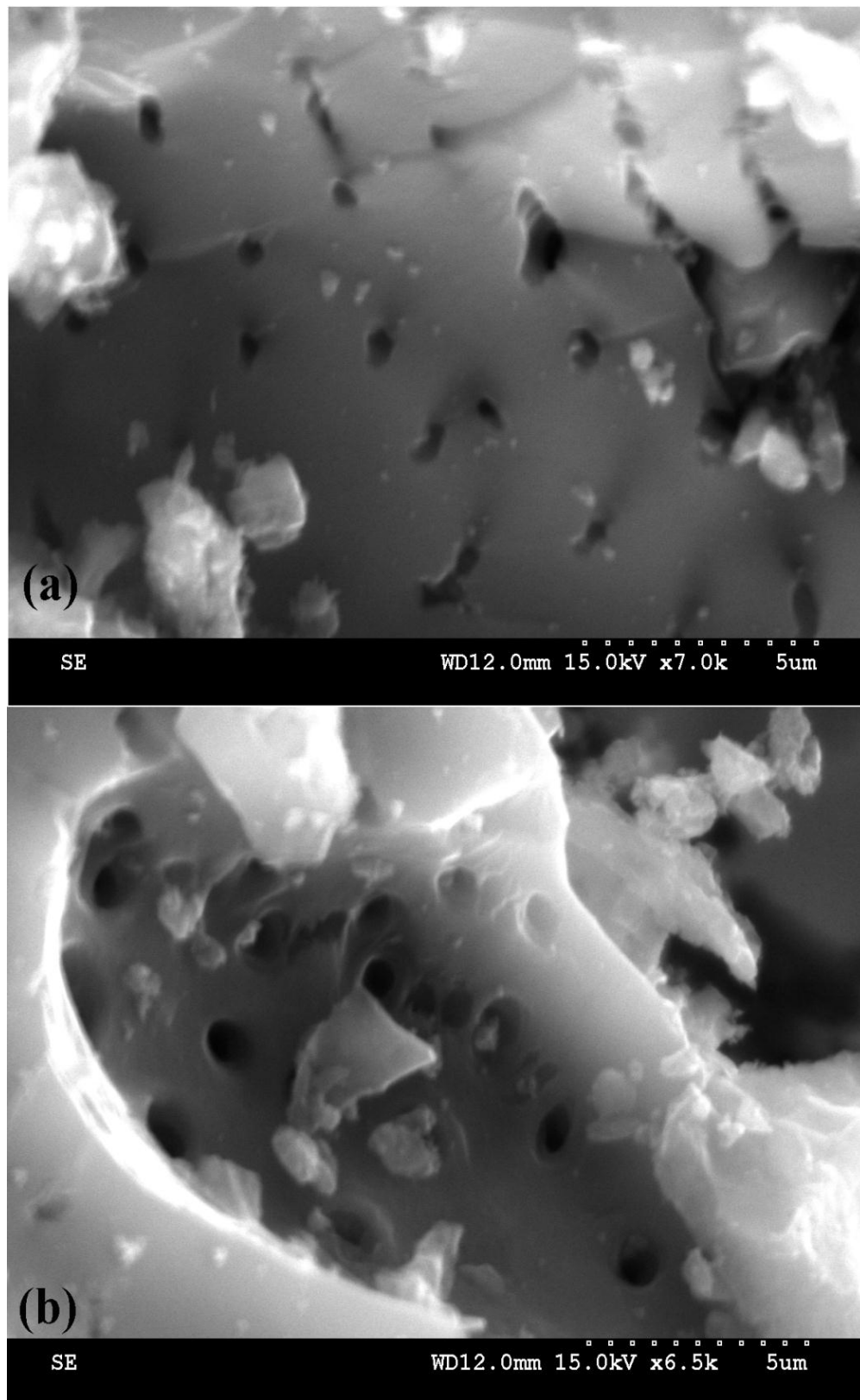


Fig. 3. SEM photographs of activated carbons (a) AC-1 and (b) AC-2

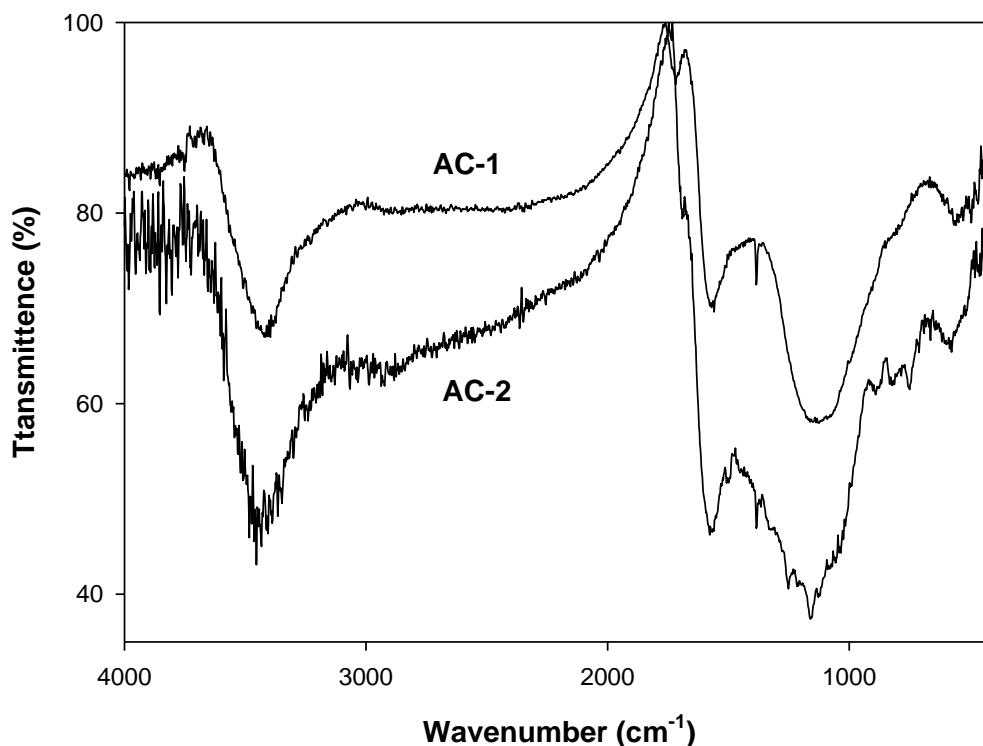


Fig. 4. FT-IR spectra for AC-1 and AC-2

The pH_{ZPC} value provides important information about the acidity and basicity of activated carbons, which has helped in the understanding of the adsorption mechanism (Cazetta *et al.* 2011). It was found that the pH_{ZPC} values were 2.12 and 5.67 for AC-1 and AC-2, respectively, demonstrating the acidic nature of the samples (Table 1). The surfaces of activated carbon acquire a positive surface charge at a solution pH lower than pH_{ZPC} and a negative surface charge when the solution pH is higher than pH_{ZPC} . Consequently, at a solution pH lower than pH_{ZPC} , theory suggests that the samples are inclined to adsorb anionic dyes due to the electrostatic interactions.

Effect of pH

The initial pH of the solution is an important parameter because it affects the adsorption capacity. As can be seen from Fig. 5(a), the highest removal of MB from the solution was 44.09% and 71.01% at pH 4.06 for AC-1 and AC-2, respectively. Above or below pH 4.06, the removal of MB presented an undesirable downward trend. This phenomenon may be interpreted as follows: at a low pH, the surface of adsorbent is protonated, and a repulsive force may develop between the positively charged adsorbent and the cationic dye of MB. In addition, hydrogen bonding formation between the activated carbon and MB is hindered at a low pH. At a high pH, the shape of the adsorbate may be the primary factor influencing the removal. However, the highest MB removal of AC-2 was observed at pH 4.06 which was lower than its pH_{zpc} value. This was an interesting phenomenon and deserves further exploration in future work.

Effect of Adsorbate Dosage

The effect of adsorbate dosage in adsorption experiments is of importance because it is closely related to the industrial application in wastewater treatment, in terms

of efficiency and economy. It can be noted from Fig. 5(b) that with the augmentation of the adsorbate dosage, greater removal of MB was obtained. The removal rate of MB increased sharply when the adsorbate dosage was increased from 0.5 g L⁻¹ to 1.0 g L⁻¹, and then approached a plateau above 1.5 g L⁻¹ for all samples. Beyond the dosage of 1.5 g L⁻¹, the increase in removal efficiency was marginal. It is known that the increase in adsorbent concentration generally results in an increase in percent adsorption of MB due to the greater availability of exchangeable sites or surface area but decreased the adsorption amount due to the partial aggregation or overlapping of activated carbon, which resulted in a decrease in effective surface area for the adsorption (Kilic *et al.* 2011). Therefore, 1.5 g L⁻¹ was found to be sufficient for MB removal in the present work.

Effect of Contact Time

An experiment on the effect of contact time was conducted in order to determine the equilibrium time required for the adsorption of MB, thus providing the shortest time needed for the adsorption. It is clearly seen from Fig. 5(c) that the adsorption reached equilibrium in 100 min, indicating that MB was removed quickly on AC-1 and AC-2. Further increase of contact time appeared to play little role in MB removal when approaching equilibrium. The fast removal of MB in the initial stage is probably due to numbers of vacant sites available for MB molecules (Acharya *et al.* 2009). However, the reason why low adsorption of MB subsequently occurred was perhaps that aggregation of MB molecules negated the influence of contact time as the micropores were filled up and started offering resistance to the diffusion of aggregated dye molecules in the adsorbents (Kumar *et al.* 2011). It can also be observed that excellent elimination capacity of MB was revealed in AC-2.

Adsorption Kinetic Studies

In order to investigate the rate-limiting step, the time-dependent experimental data were analyzed by fitting them to different kinetic models, namely the pseudo-first order model, the pseudo-second order model, and the intraparticle diffusion model.

Pseudo-first order model

Since it was first put forward by Lagergren, the pseudo-first order kinetic model has been employed to extensively study the kinetics of adsorption. The linear form of the pseudo-first order is represented by,

$$\ln(q_e - q_t) = \ln q_e - K_1 t \quad (5)$$

where K_1 (min⁻¹) is the rate constant of the pseudo-first order.

Pseudo-second order model

The pseudo-second order model equation can be expressed as,

$$t/q_t = 1/(K_2 q_e^2) + t/q_e \quad (6)$$

where K_2 is the rate constant of the pseudo-second order.

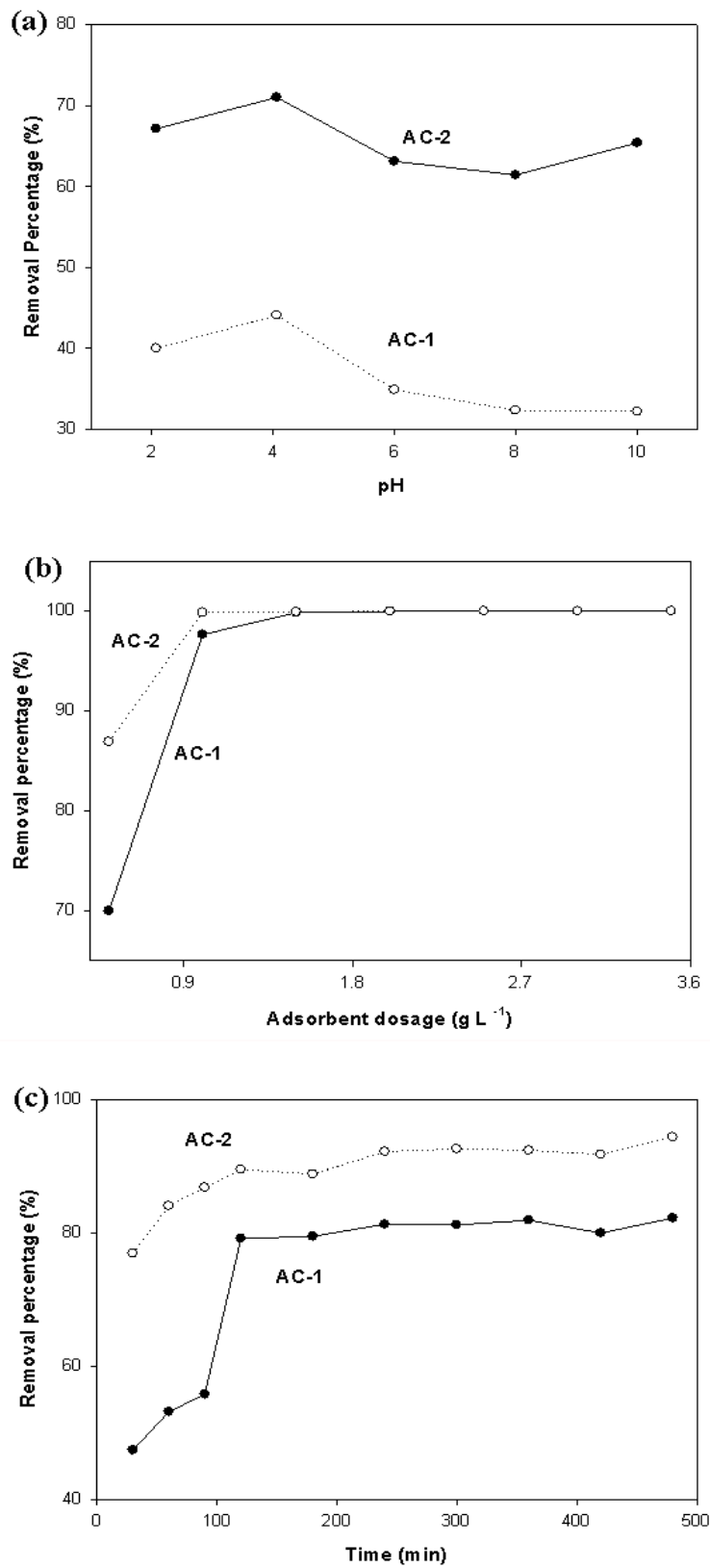


Fig. 5. Effect of pH, adsorbent dosage, and time

Parameters and correlation coefficients (R^2) are presented in Table 2. The R^2 values of the pseudo-second order model for AC-1 and AC-2 were 0.9999 and 1.000, respectively. Both values were higher than for the pseudo-first order model, indicating a much better fit. This suggests that the rate-controlling step of adsorption of MB was largely attributable to chemical sorption. Additionally, the q_e values for AC-1 and AC-2, calculated from pseudo-second order model, were 193.8 mg g^{-1} and 200.4 mg g^{-1} , respectively. These were consistent with the experimental data 192.1 mg g^{-1} and 199.5 mg g^{-1} , demonstrating that the pseudo-second order model provided a better fit for the adsorption of MB as well. The applicability of the pseudo-second order model means the rate of adsorption was subject to a second order rate law, with respect to the availability of adsorption sites on the surface of adsorbent rather than adsorbate concentration in bulk solution (Liu 2008). By comparing the results of K_2 values for AC-1 (0.001512 $\text{g mg}^{-1} \text{min}^{-1}$) with those of AC-2 (0.004494 $\text{g mg}^{-1} \text{min}^{-1}$), it was found that AC-2 showed a quicker MB adsorption rate under the same experimental conditions.

Table 2. Kinetic Model Parameters and Correlation Coefficients for Adsorption of MB onto AC-1 and AC-2

Kinetic model	Parameter	AC-1	AC-2
Pseudo-first order	K_1 (min^{-1})	0.01262	0.02172
	q_e (mg g^{-1})	21.37	11.39
	R^2	0.9652	0.9796
Pseudo-second order	K_2 (g (mg min)^{-1})	0.001512	0.004494
	q_e (mg g^{-1})	193.8	200.4
	R^2	0.9999	1.000
Intraparticle diffusion model	K_p	1.6576	0.7728
	C	167.94	189.1
	R^2	0.8835	0.6909
	$q_{e,\text{exp}}$ (mg g^{-1})	192.1	199.5

Intraparticle diffusion model

Though the pseudo-first-order model and the pseudo-second-order model are widely applied to study kinetic adsorption, it is known that they are not suitable to explain the diffusion mechanism occurring in the adsorption process, which is generally the rate-determining step. Thus, the intraparticle diffusion model was introduced to give explicit information about the diffusion mechanism. The equation is expressed as,

$$q_t = K_p t^{0.5} + C \quad (7)$$

where K_p represents the rate constant ($\text{mg g}^{-1} \text{min}^{-0.5}$). C (mg g^{-1}) is a constant that reflects the significance of the boundary layer or mass transfer effect.

According to the model, if the plot of q_t vs. $t^{0.5}$ is a straight line and the plot passed through the origin, then the sorption process is controlled by only intraparticle diffusion (Ren *et al.* 2011). It can be observed from Fig. 6 that the plots were not completely linear and did not pass through the origin, which indicated that intraparticle diffusion was not the sole rate-controlling step and that boundary layer diffusion made some contribution. Generally speaking, plots showed three features: an initial curved portion, followed by a linear portion, and a plateau. Judging from the plots shown in Fig.

9, a dual nature was represented. The initial curved portion was not observed from the plots, and this is probably attributable to the fast movement of MB molecules from the solution towards the external surface of the activated carbon. The intermediate linear portion of the plot was due to intraparticle diffusion and the following plateau to the equilibrium stage where intraparticle diffusion started to slow down due to extremely low solute concentrations in the solution (Daifullah *et al.* 2007).

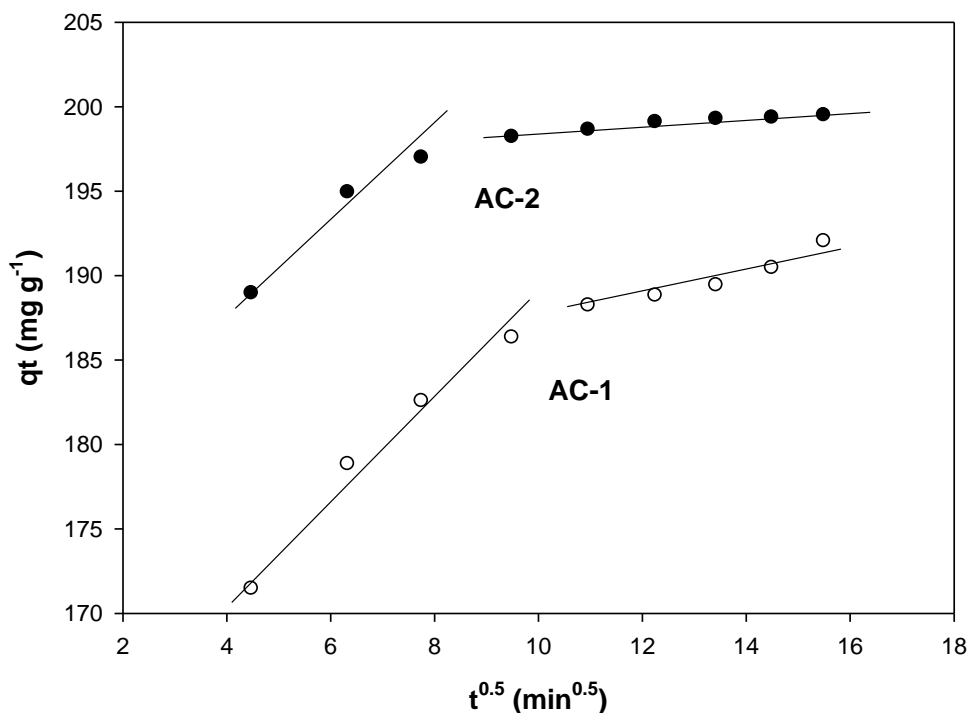


Fig. 6. Intraparticle diffusion plot for the adsorption of MB on AC-1 and AC-2

Adsorption Equilibrium Studies

Adsorption isotherms were employed to illustrate how the adsorbate molecules distribute between the liquid phase and the solid phase and are important for the design of the adsorption system. In this work, the adsorption equilibrium data were modeled to the Freundlich isotherm and Langmuir isotherm.

Freundlich isotherm

The Freundlich isotherm is an empirical model that is based on adsorption on a heterogeneous surface and active sites with different energies (Kilic *et al.* 2011). The linear form of the Freundlich isotherm is given by the following equation,

$$\log q_e = \log K_f + \frac{1}{n} \log C_e \quad (8)$$

where n and K_f ((mg g⁻¹) (L mg⁻¹)^{1/n}) are Freundlich constants related to the favorability of adsorption process and the adsorption capacity of the adsorbate, respectively. If the value of $1/n$ is less than 1, it indicates favorable adsorption.

Table 3 lists all the parameters and coefficients of determination (R^2) for adsorption of MB onto AC-1 and AC-2. For the Freundlich isotherm, it was found that the values of n were 5.7 and 6.3 for AC-1 and AC-2, respectively, indicating that both of

the adsorption processes were favorable. According to the theory, the higher the value of the exponent n , the higher will be the affinity and the heterogeneity of the adsorbent sites (Srivastava *et al.* 2006). The conclusion can be drawn that AC-2 displayed stronger affinity and greater heterogeneity for MB than AC-1.

Table 3. Isotherm Model Parameters and Correlation Coefficients for Adsorption of MB onto AC-1 and AC-2

Isotherm model	Parameter	AC-1	AC-2
Freundlich	$K_f ((\text{mg g}^{-1}) (\text{L mg}^{-1})^{1/n})$	136.8	193.8
	n	5.7	6.3
	R^2	0.9024	0.8586
Langmuir	$q_m (\text{mg g}^{-1})$	291.5	342.5
	$K_L (\text{L mg}^{-1})$	0.4188	1.062
	R^2	0.9895	0.9931

Langmuir isotherm

The Langmuir isotherm model suggests monolayer sorption on a homogeneous surface without interaction between the sorbed molecules and uniform energies of sorption onto the surface, with no transmigration of the sorbate (Vimala and Das 2009). The model is represented by the following equation,

$$\frac{c_e}{q_e} = \frac{1}{q_m K_L} + \frac{c_e}{q_m} \quad (9)$$

where $q_m (\text{mg g}^{-1})$ and $K_L (\text{L mg}^{-1})$ are Langmuir constants related to adsorption capacity and rate of adsorption, respectively.

Table 4. Comparison of Maximum Monolayer Adsorption of MB onto Activated Carbons from Different Precursors

Precursor	Agent	Adsorption capacity (mg g^{-1})	Reference
Sunflower oil cake	H_2SO_4	16.43	Karagöz <i>et al.</i> 2008
Oil palm fiber	KOH	382.32	Foo and Hameed 2012
Cashew nut shell	KOH	68.72	Kumar <i>et al.</i> 2011
Pine wood powder	ZnCl_2	200.00	Wang <i>et al.</i> 2009
Bamboo	H_3PO_4	286.10	Liu <i>et al.</i> 2010
Cotton stalk	ZnCl_2	315.45	Deng <i>et al.</i> 2009
<i>Posidonia oceanica</i> dead leaves	ZnCl_2	285.71	Dural <i>et al.</i> 2011
Jute fiber	H_3PO_4	225.64	Senthilkumaar <i>et al.</i> 2005
Tea fruit peel residues	$\text{H}_3\text{PO}_4/\text{ZnCl}_2$	291.5/342.5	Present study

Based on the R^2 shown in Table 3, it can be concluded that the Langmuir model produced the better fit to the experimental data with higher R^2 for both AC-1 (0.9895) and AC-2 (0.9931), which suggested that the adsorption was a process occurring in a homogeneous surface with uniform energies and there was no transmigration of the MB dyes. In other words, this was an indication of the formation of monolayer coverage of

MB molecules on the accessible surfaces of the activated carbon. In addition, the maximum adsorption capacities determined from the Langmuir model were 291.5 mg g^{-1} and 342.5 mg g^{-1} for AC-1 and AC-2, respectively. These are in good agreement with the experimental observation, which further demonstrated that the adsorption process complied with the Langmuir model. For the sake of comparison, Table 4 lists the maximum monolayer adsorption of MB onto activated carbons prepared from different precursors. It was found that activated carbons fabricated by H_3PO_4 and ZnCl_2 from tea peel fruit residues presented good performance for the adsorption of MB.

CONCLUSIONS

1. Activated carbons with large surface areas ($1024.19 \text{ m}^2 \text{ g}^{-1}$ and $1320.22 \text{ m}^2 \text{ g}^{-1}$) and total pore volumes ($0.7463 \text{ cm}^3 \text{ g}^{-1}$ and $0.7854 \text{ cm}^3 \text{ g}^{-1}$) were obtained using the agents ZnCl_2 or H_3PO_4 .
2. Equilibrium adsorption studies indicated that the adsorption process was favorable and the maximum monolayer adsorption capacities of methylene blue were 291.5 and 342.5 mg g^{-1} , respectively, for AC-1 and AC-2.
3. Both AC-1 and AC-2 showed rapid removal of MB, however, by comparing AC-1 with AC-2, it can be concluded that AC-2 exhibited an excellent physical structure and greater removal of MB from the solution.

ACKNOWLEDGMENTS

This work was supported by the Ministry of Science and Technology, PR China (No. 2011BAD01B03-5-1).

REFERENCES CITED

- Acharya, J., Sahu, J., Mohanty, C., and Meikap, B. (2009). "Removal of lead (II) from wastewater by activated carbon developed from *Tamarind wood* by zinc chloride activation," *Chem. Eng. J.* 149(1), 249-262.
- Ahmaruzzaman, M. (2008). "Adsorption of phenolic compounds on low-cost adsorbents: A review," *Adv. Colloid Interfac.* 143(1), 48-67.
- Baccar, R., Bouzid, J., Feki, M., Montiel, A. (2009). "Preparation of activated carbon from Tunisian olive-waste cakes and its application for adsorption of heavy metal ions," *J. Hazard. Mater.* 162(2), 1522-1529.
- Cazetta, A. L., Vargas, A. M. M., Nogami, E. M., Kunita, M. H., Guilherme, M. R., Martins, A. C., Silva, T. L., Moraes, J. C. G., and Almeida, V. C. (2011). "NaOH-activated carbon of high surface area produced from coconut shell: Kinetics and equilibrium studies from the methylene blue adsorption," *Chem. Eng. J.* 174(1), 117-125.
- Crini, G. (2006). "Non-conventional low-cost adsorbents for dye removal: A review," *Bioresour. Technol.* 97(9), 1061-1085.

- Cuhadaroglu, D., and Uygun, O. (2008). "Production and characterization of activated carbon from a bituminous coal by chemical activation," *Afr. J. Biotechnol.* 7(20), 3703-3710.
- Daifullah, A. A., Yakout, S. M., and Elreefy, S. A. (2007). "Adsorption of fluoride in aqueous solutions using KMnO₄-modified activated carbon derived from steam pyrolysis of rice straw," *J. Hazard. Mater.* 147(1-2), 633-643.
- Demirbas, A. (2009). "Agricultural based activated carbons for the removal of dyes from aqueous solutions: A review," *J. Hazard. Mater.* 167(1), 1-9.
- Deng, H., Yang, L., Tao, G., and Dai, J. (2009). "Preparation and characterization of activated carbon from cotton stalk by microwave assisted chemical activation-application in methylene blue adsorption from aqueous solution," *J. Hazard. Mater.* 166(2), 1514-1521.
- Dural, M. U., Cavas, L., Papageorgiou, S. K., and Katsaros, F. K. (2011). "Methylene blue adsorption on activated carbon prepared from *Posidonia oceanica* (L.) dead leaves: Kinetics and equilibrium studies," *Chem. Eng. J.* 168(1), 77-85.
- Foo, K. Y., and Hameed, B. H. (2012). "Adsorption characteristics of industrial solid waste derived activated carbon prepared by microwave heating for methylene blue," *Fuel Process. Technol.* 99, 103-109.
- Foo, K. Y., and Hameed, B. H. (2011a). "Microwave-assisted preparation and adsorption performance of activated carbon from biodiesel industry solid residue: Influence of operational parameters," *Bioresour. Technol.* 103(1), 398-404.
- Foo, K. Y., and Hameed, B. H. (2011b). "Microwave-assisted preparation of oil palm fiber activated carbon for methylene blue adsorption," *Chem. Eng. J.* 166(2), 792-795.
- Garg, V., Amita, M., Kumar, R., and Gupta, R. (2004). "Basic dye (methylene blue) removal from simulated wastewater by adsorption using Indian rosewood sawdust: A timber industry waste," *Dyes Pigments* 63(3), 243-250.
- Gupta, V. (2009). "Application of low-cost adsorbents for dye removal- A review," *J. Environ. Manage.* 90(8), 2313-2342.
- Karagöz, S., Tay, T., Ucar, S., and Erdem, M. (2008). "Activated carbons from waste biomass by sulfuric acid activation and their use on methylene blue adsorption," *Bioresour. Technol.* 99(14), 6214.
- Kilic, M., Apaydin-Varol, E., and Pütün, A.E. (2011). "Adsorptive removal of phenol from aqueous solutions on activated carbon prepared from tobacco residues: Equilibrium, kinetics and thermodynamics," *J. Hazard. Mater.* 189(1), 397-403.
- Kumar, P. S., Ramalingam, S., and Sathishkumar, K. (2011). "Removal of methylene blue dye from aqueous solution by activated carbon prepared from cashew nut shell as a new low-cost adsorbent," *Korean J. Chem. Eng.* 28(1), 149-155.
- Kyzas, G. Z., Lazaridis, N. K., and Mitropoulos, A. C. (2012). "Removal of dyes from aqueous solutions with untreated coffee residues as potential low-cost adsorbents: Equilibrium, reuse and thermodynamic approach," *Chem. Eng. J.* 189-190, 148-159.
- Liou, T. H. (2010). "Development of mesoporous structure and high adsorption capacity of biomass-based activated carbon by phosphoric acid and zinc chloride activation," *Chem. Eng. J.* 158(2), 129-142.
- Liu, Q. S., Zheng, T., Wang, P., Jiang, J. P., and Li, N. (2010). "Adsorption isotherm, kinetic and mechanism studies of some substituted phenols on activated carbon fibers," *Chem. Eng. J.* 157(2), 348-356.

- Liu, Y. (2008). "New insights into pseudo-second-order kinetic equation for adsorption," *Colloid. Surface. A* 320(1-3), 275-278.
- Ma, J., Jia, Y., Jing, Y., Yao, Y., and Sun, J. (2011). "Kinetics and thermodynamics of methylene blue adsorption by cobalt-hectorite composite," *Dyes Pigments* 93(1-3), 1441-1446.
- Moreno-Castilla, C. (2004). "Adsorption of organic molecules from aqueous solutions on carbon materials," *Carbon* 42(1), 83-94.
- Nieto-Delgado, C., Terrones, M., and Rangel-Mendez, J. (2011). "Development of highly microporous activated carbon from the alcoholic beverage industry organic by-products," *Biomass Bioenergy* 35(1), 103-112.
- Ren, L., Zhang, J., Li, Y., and Zhang, C. (2011). "Preparation and evaluation of cattail fiber-based activated carbon for 2, 4-dichlorophenol and 2, 4, 6-trichlorophenol removal," *Chem. Eng. J.* 168(2), 553-561.
- Sahu, J. N., Acharya, J., and Meikap, B. C. (2010). "Optimization of production conditions for activated carbons from tamarind wood by zinc chloride using response surface methodology," *Bioresour. Technol.* 101(6), 1974-1982.
- Senthilkumar, S., Varadarajan, P., Porkodi, K., and Subbhuraam, C. (2005). "Adsorption of methylene blue onto jute fiber carbon: kinetics and equilibrium studies," *J. Colloid Interf. Sci.* 284(1), 78-82.
- Srivastava, V. C., Mall, I. D., and Mishra, I. M. (2006). "Equilibrium modelling of single and binary adsorption of cadmium and nickel onto bagasse fly ash," *Chem. Eng. J.* 117(1), 79-91.
- Vargas, A. M. M., Cazetta, A. L., Kunita, M. H., Silva, T. L., and Almeida, V. C. (2011). "Adsorption of methylene blue on activated carbon produced from flamboyant pods (*Delonix regia*): Study of adsorption isotherms and kinetic models," *Chem. Eng. J.* 168(2), 722-730.
- Vimala, R., and Das, N. (2009). "Biosorption of cadmium (II) and lead (II) from aqueous solutions using mushrooms: A comparative study," *J. Hazard. Mater.* 168(1), 376-382.
- Wang, S., Boyjoo, Y., Choueib, A., and Zhu, Z. (2005). "Removal of dyes from aqueous solution using fly ash and red mud," *Water Res.* 39(1), 129-138.
- Wang, T., Tan, S., and Liang, C. (2009). "Preparation and characterization of activated carbon from wood via microwave-induced ZnCl₂ activation," *Carbon* 47(7), 1880-1883.

Article submitted: January 14, 2013; Peer review completed: February 10, 2013; Revised version received and accepted: February 26, 2013; Published: March 5, 2013.